A LETTERS JOURNAL EXPLORING THE FRONTIERS OF PHYSICS

OFFPRINT

Overlapping of acoustic bandgaps using fractal geometries

S. CASTIÑEIRA-IBÁÑEZ, V. ROMERO-GARCÍA, J. V. SÁNCHEZ-PÉREZ and L. M. GARCIA-RAFFI

EPL, **92** (2010) 24007

A Letters Journal Exploring the Frontiers of Physics

October 2010

EPL, **92** (2010) 24007
doi: 10.1209/0295-5075/92/24007

www.epljournal.org

Overlapping of acoustic bandgaps using fractal geometries

S. Castiñeira-Ibáñez[1], V. Romero-García[2,3], J. V. Sánchez-Pérez[3(a)] and L. M. Garcia-Raffi[4]

[1] *Departamento de Física Aplicada, Universidad Politécnica de Valencia - Camino de Vera s/n, 46022 Valencia, Spain, EU*
[2] *Instituto de Ciencia de Materiales, CSIC - Sor Juana Inés de la Cruz, 3, Cantoblanco, 28049 Madrid, Spain, EU*
[3] *Centro de Tecnologías Físicas: A.M.A., Universidad Politécnica de Valencia - Camino de Vera s/n, 46022 Valencia, Spain, EU*
[4] *Instituto Universitario de Matemática Pura y Aplicada, Universidad Politécnica de Valencia - Camino de Vera s/n, 46022 Valencia, Spain, EU*

received 21 June 2010; accepted in final form 11 October 2010
published online 15 November 2010

PACS 43.20.+g – General linear acoustics
PACS 43.35.+d – Ultrasonics, quantum acoustics, and physical effects of sound

Abstract – The transmission of acoustic waves in a fractal distribution of rigid scatterers embedded in air is reported in this work. The Sierpinsky fractal is used to produce a compact small device containing several periodicities, therefore the fractal distribution contains several finite sonic crystals. The attenuation band produced by the fractal distribution results from the sum of the Bragg peaks of each periodicity. On the other hand, bandgaps of sonic crystal depend on the well-known filling fraction, thus the radii of the scatterers in the fractal distribution has been optimized using genetic algorithm in order to overlap the bandgaps of each periodicity obtaining a wide and full attenuation band.

Research into heterogeneous artificial materials, consisting of arrangements of rigid scatterers embedded in a medium with different elastic properties, has been intensely developed throughout the last two decades. The capability to prevent the transmission of waves in predetermined bands of frequencies —called bandgaps— is one of the most interesting properties of these systems, and leads to the possibility of designing devices to control the wave propagation. The underlying physical mechanism is the destructive Bragg interference. Here we show a technique that enables the creation of a wide attenuation band in these materials, based on fractal geometries. We have focused our work in the acoustic case where these materials are called Phononic/Sonic Crystals (SC) [1,2] but the technique could be applied to any type of crystals and waves in ranges of frequencies where the physics of the process is linear.

Composites made of acoustically hard cylinders (scatterers) periodically embedded in air (host) are characterized by a large acoustic mismatch between the cylinder and substrate materials, therefore modes of acoustic waves are not allowed to exist in the cylinders and the physical problem is reduced to the scattering based on Bragg's law. With these conditions, the position and the size of the bandgaps in the range of frequencies depend on: a) the arrangement of the scatterers, according to the Bragg's law and b) the amount of matter formed by the scatterers, quantified by the filling fraction (ff). For a given SC, the range of frequencies of the bandgap can only get wider by increasing the ff.

In the last years two ways for changing the characteristics of full SC bandgaps have mainly been developed [3,4]. First, by varying the intrinsic acoustical properties of the scatterers [5–7] and, second, by developing new arrangements of scatterers different from the crystalline symmetries. Quasi-crystals [8] and Quasi-Ordered Structures [9] are examples of this second strategy. Recently new arrangements of scatterers characterized by the concept of hyperuniformity, have been used to obtain large and complete bandgaps with amorphous photonic materials [10]. Here, we propose a new procedure to obtain large attenuation bands based on the redistribution of the elements of the SC based on fractal geometries [11]. We have chosen these geometries because they can be modelled mathematically and they can be used as design tools. Recently fractals have been under study for a wide range of practical applications, from biological or medical [12] to economics [13]. However, fractals have

(a) E-mail: jusanc@fis.upv.es

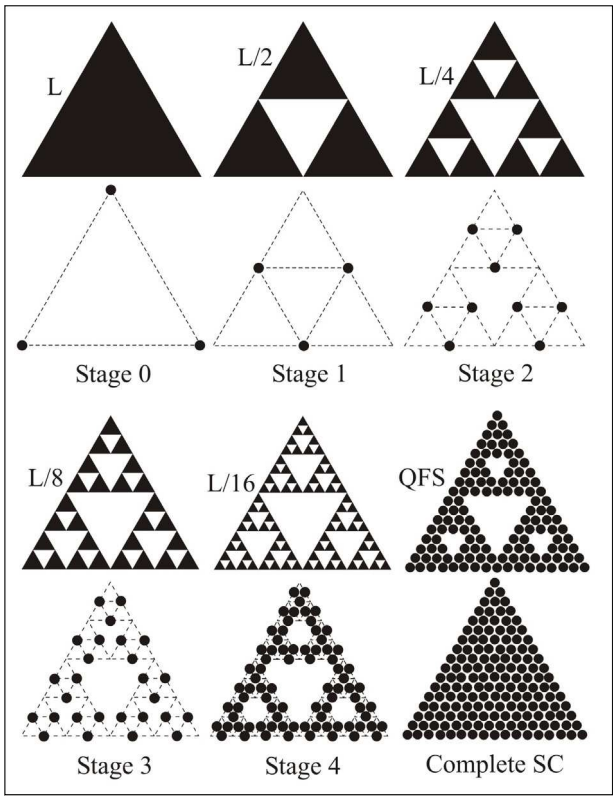

Fig. 1: Quasi-fractal arrangement of scatterers: Five stages of cylinder arrays based on Sierpinski's triangle geometry and the resulting complete SC and QFS structure.

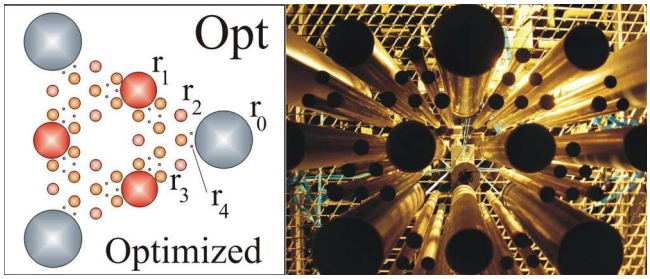

Fig. 2: (Colour on-line) Left: optimized arrangement of scatterers based on the Sierpinski triangle with different relationships among the radii of the cylinders (QFS_{Opt}). Right: photograph taken from beneath the commercial arrangement (QFS_{Exp}) used to validate theoretical results. Part of the supporting frame can be seen, too.

only been used in the field of SC [14–17] to design the shapes of the scatterers [18].

The first step we have considered is the design of an arrangement of scatterers inside an equilateral triangle of side L based on a 2D fractal called Sierpinsky triangle (see fig. 1). We have chosen a 2D symmetry triangular pattern because among the other periodicities it presents the largest bandgap as a consequence of its degree of hyperuniformity [10]. In fig. 1, we represent a transversal section (in the XY plane) of our arrangement considering infinitely long cylinders with radius r parallel to the z-axis. We have called it Quasi-Fractal Structure (QFS) because, although the fractal construction follows an infinite iterative process [11], we only show here the first five iterations (or stages). The QFS shown here is constrained by both L and r. Figure 1 also shows that one cylinder is located at every vertex of the empty triangles (white triangle) in each stage, except at stage zero where the scatterers are located at the vertex of the existing triangle (Black triangle). Also, one can compare in fig. 1 the complete SC and the QFS resulting from the sum of the different stages. At first glance one might consider that the QFS is a classical triangular crystalline array with some vacancies in its structure. However, the underlying symmetry follows a fractal pattern. Thus, we can consider the QFS as a sum of independent triangular arrays with different lattice constants (L, $L/2$, $L/4$, $L/8$ and $L/16$), with every stage located iteratively within the previous one. This provides a compact small device whose attenuation band results from the sum of the Bragg peak corresponding to the periodicity of each stage. This idea is consistent with the nature of fractal geometries which are based on the repetition of identical motifs at differing size scales [11].

The relationship between the different lattice constants of each stage in the QFS can also be used to explain the existence of a large full attenuation band. As one can observe in fig. 1 the lattice constants are proportional to $1/2^M$, M being the order number of the stage. This produces an overlapping of many Bragg peaks at different stages and a reinforcement of the attenuation bands. It is possible to find an expression to obtain the number of repeated Bragg peaks at different stages. The following functions $S_\alpha(n, M)$, $\alpha = 0°$, $30°$ give the value of the frequency for which the n-th Bragg peak appears at the different stages M ($M = 0$, 1, 2, 3, 4), as a function of L and along the two high-symmetry directions of the triangular array (0°, 30°)

$$\begin{aligned} S_{0°}(n, M) &= C_{0°}(n+1)2^M, \\ S_{30°}(n, M) &= C_{30°}(n+2)2^{M-1}, \end{aligned} \tag{1}$$

where $C_{0°} = \sqrt{3}/3$ and $C_{30°} = 2/3$ due to the Bragg law. Based on eqs. (1), it is straightforward to find the relationship of the appearance of a predetermined Bragg peak for any two different stages:

$$\begin{aligned} (0°) \quad n &= (n'+1)2^V - 1, \\ (30°) \quad n &= (n'+2)2^V - 2, \end{aligned} \tag{2}$$

where V is the difference between the couple of stages we want to compare ($V = 1$, 2, 3, 4). Equations (2) show the relationship between the n-position of the appearance of a Bragg peak in the stage M as a function of the n'-position of the appearance of the same peak in another stage M', such that $V = M' - M$. Note the large number of

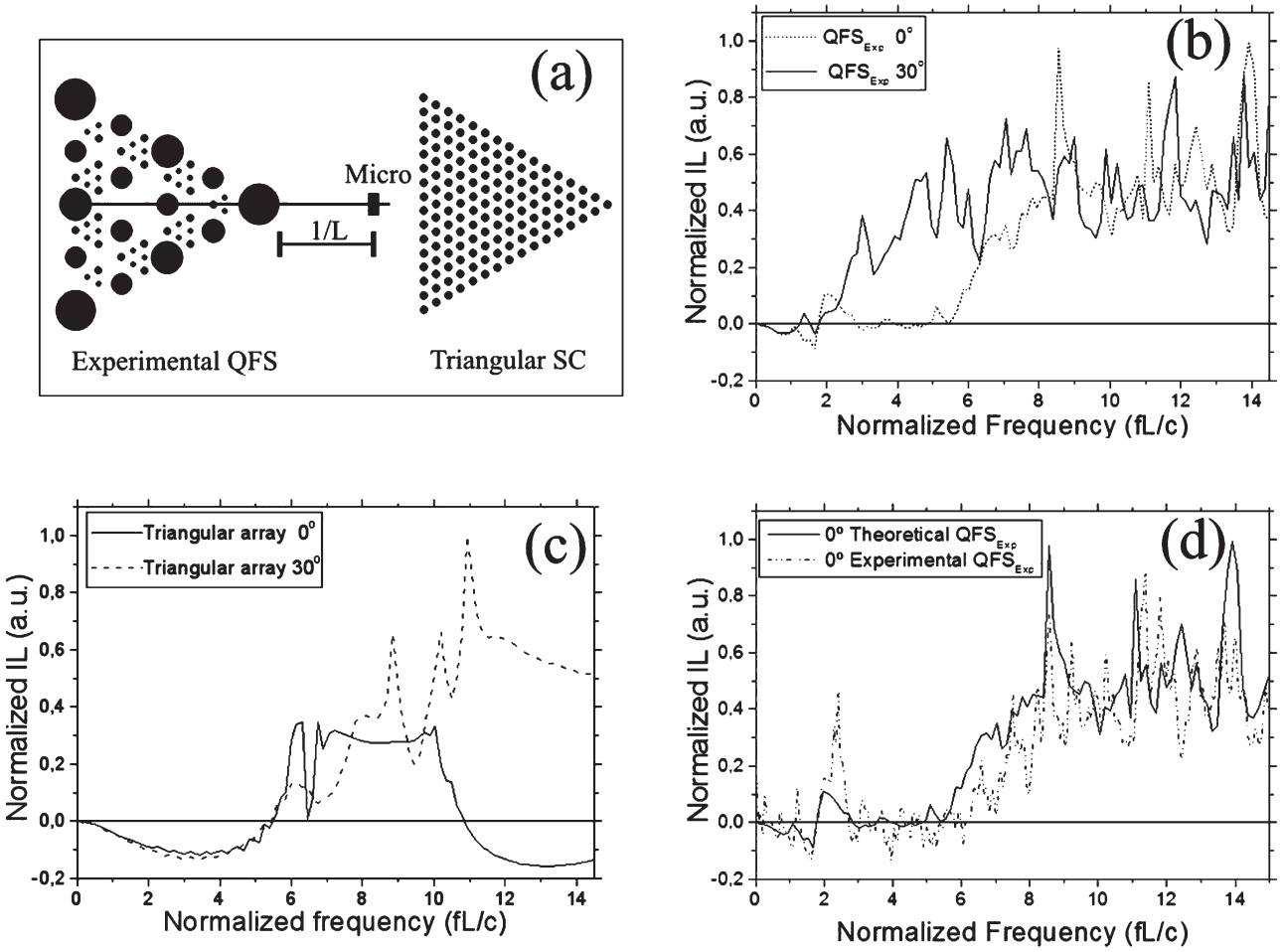

Fig. 3: Attenuation properties of the designed devices: (a) experimental Quasi-Fractal Structure ($\mathrm{QFS_{Exp}}$) and the triangular SC used. The relationship among the radii of the cylinders for the first case is ($r_0/L \approx 0.094$; $r_1/L \approx 0.078$; $r_2/L \approx 0.054$; $r_3/L \approx 0.029$; $r_4/L \approx 0.017$), being ($\mathrm{ff_{Exp}} = 33\%$). (b) Theoretical normalized IL spectra along the two high-symmetry directions for $\mathrm{QFS_{Exp}}$. (c) The same for the triangular array ($\mathrm{ff_{SC}} = 36\%$). (d) Both Theoretical and Experimental $\mathrm{QFS_{Exp}}$ attenuation spectra for the ΓX-direction.

times certain Bragg peaks are repeated on different stages according to eq. (2), producing a reinforcement and, as a consequence, an enhancement of the full attenuation band. We want to point out that the above formulas are valid if the considered stage has a minimum number of cells.

The second step constitutes an important part of our design technique. We have designed the diameter of each set of cylinders in each stage independently in order to distribute the filling fraction of each stage in a more efficient way: increasing the sizes in the low stages and reducing them in the higher ones, thereby providing each stage with the adequate value of ff for the appearance of their Bragg's peaks. As a consequence, a further increase of the attenuation band occurs. In fig. 2 we show a proposed QFS built with an optimized relationship between the radii of the cylinders belonging to the different stages M ($M = 0$, 1, 2, 3, 4). For the optimization process we have used genetic algorithm previously adapted to the acoustic case [9]. The cylinders of the optimized QFS ($\mathrm{QFS_{Opt}}$) present the following radii for each stage: $r_0/L \approx 0.14$, $r_1/L \approx 0.09$, $r_2/L \approx 0.03$, $r_3/L \approx 0.032$ and $r_4/L \approx 0.02$. We would like to point out that it has been necessary to remove some cylinders of the starting QFS shown in fig. 1 in order to place the biggest cylinders (large radii) of the first stages. Of course, other relationships among the radii of the cylinders could be appropriate for other applications.

To quantify the size of the attenuation band of this device we have used the Attenuation Area (AA) parameter in the analyzed range of frequencies and, at the moment, only along the ΓX-direction (0° degrees). The AA parameter has been used successfully in previous works [9] to obtain the attenuation power of a SC in a predetermined range of frequencies. It is defined as the area enclosed between the positive Insertion Loss (IL) spectra and the 0 dB threshold in the frequency range selected. Comparing the AA value for the $\mathrm{QFS_{Opt}}$ with the corresponding to a SC with the same external size and shape, and made of rigid cylinders (radius $r/L \approx 0.02$) arranged in triangular lattice, we obtain interesting results: the AA parameter grows for the $\mathrm{QFS_{Opt}}$ case ($\mathrm{AA_{Opt}} = 179.88$ arbitrary units) more than 400% compared with the

classical triangular lattice ($AA_{SC} = 43.94$ a.u.). We would like to note that QFS_{Opt} has been designed under the premise of maintaining the same ff as SC ($ff_{Opt} = ff_{SC} = 36\%$). With these data, we can break the rule about the relationship between ff and the size of the bandgaps: we have obtained a high increase in the size of the attenuation band without increasing the ff of the device with respect to the original triangular array device. These results have been calculated in the normalized range of frequencies 0–15 shown in fig. 3. Also, we have normalized the IL of each spectrum with its maximum value of IL in order to obtain the AA in arbitrary units. We want to point out the fact that the obtained results are valid for every range of frequencies where the behavior of the system is linear. Moreover, due to the nature of our technique, the crystal wave properties of our device remain intact for each stage as it is a sum of triangular arrays. This means that the attenuation band obtained along the other high-symmetry direction, ΓJ (30°) and the full attenuation band of the QFS also grow comparing to the corresponding bandgap and full bandgap of the SC, respectively (the full attenuation band of the QFS is 200% higher than the full bandgap of the SC).

To illustrate the above statement experimentally we have constructed a new device similar to QFS_{Opt} but with commercially available hollow cylinders, QFS_{Exp} (fig. 3(a)). In figs. 3(b), (c) one can compare the theoretical normalized IL spectra, along the two high-symmetry directions ΓX and ΓJ (0°, 30°), for both QFS_{Exp} and the SC defined above. The difference in the size of the bandgaps in fig. 3(c) for 0 and 30 degrees can be explained in terms of the external shape of the designed device: for the triangular external shape, a constructive interference area appears in front of the vertex of the triangle [19]. As a consequence, a reduction in the size of the bandgap at 0° appears. This effect does not clearly appear at 30° of incidence. We have used Multiple Scattering Theory [20, 21] to obtain these spectra, which have been calculated at a distance $d = 1/L$ from the vertex of the sample at 0°. Moreover, in fig. 3(d) we show the good agreement between the theoretical and experimental results for 0° incidence.

In summary, in this work we have shown that an optimised fractal-based design technique enables a large increase of the attenuation bands for arrays of rigid scatterers. There are two steps. The first one consists of using fractal patterns to arrange the scatterers. The resulting device, the QFS, can be considered as the sum of several independent crystalline arrays. The second step consists of optimising the QFS by varying the ff of each fractal stage independently. As a result, we have obtained efficient and compact devices. The sum of the Bragg peaks belonging to the different scale arrays (stages), the reinforcement process due to the existence of different lattice constants and the redistribution of cylinders among the different stages are behind this enhancement.

* * *

This work was supported by MCI (Spanish Government) and FEDER funds, under Grant Nos. MAT2009-09438 and MTM2009-14483-C02-02. The authors would like to thank Prof. K. Attenborough and Dr. E. A. Sánchez-Pérez for their suggestions and for the revision of the manuscript.

REFERENCES

[1] Martínez-Sala R., Sancho J., Sánchez-Pérez J. V., Gómez V., Llinares J. and Meseguer F., *Nature*, **378** (1995) 241.
[2] Sánchez-Pérez J. V., Caballero D., Martínez-Sala R., Rubio C., Sánchez-Dehesa J., Meseguer F., Llinares J. and Gálvez F., *Phys. Rev. Lett.*, **80** (1998) 5325.
[3] Khelif A., Wilm M., Laude V., Ballandras S. and Djafari-Rouhani B., *Phys. Rev. E*, **69** (2004) 067601.
[4] Sánchez-Pérez J. V., Rubio C., Martínez-Sala R., Sánchez-Grandia R. and Gómez V., *Appl. Phys. Lett.*, **81** (2002) 5240.
[5] Umnova O., Attenborough K. and Linton C. M., *J. Acoust. Soc. Am.*, **119** (2006).
[6] Liu Z., Zhang X., Mao Y., Zhu Y., Yang Z., Chan C. and Sheng P., *Science*, **289** (2000) 1734.
[7] Kuang W., Hou Z. and Liu Y., *Phys. Lett. A*, **332** (2004) 481.
[8] Zhang X., *Phys. Rev. B*, **75** (2007) 024209.
[9] Romero-García V., Fuster E., Garcia-Raffi L. M., Sánchez-Pérez E. A., Sopena M., Llinares J. and Sánchez-Pérez J. V., *Appl. Phys. Lett.*, **88** (2006) 174104.
[10] Florescu M., Torquato S. and Steindhardt P., *Proc. Natl. Acad. Sci. U.S.A.*, **106** (2009) 20658.
[11] Mandelbrot B., *The Fractal Geometry of the Nature* (W. H. Freeman & Co., New York) 1983.
[12] Iannaccone P. M. and Khokha M., *Fractal Geometry in Biological Systems: An Analytical Approach* (CRC Press, Inc.) 1996.
[13] Williams B. and Trading B., *Chaos: Applying Expert Techniques to Maximize Your Profits* (Market place Books, Inc.) 1995.
[14] Frezza F., Pajewski L. and Schettini G., *IEEE Trans. Microwave Theory Tech.*, **52** (2004) 220.
[15] Liang L., *Chin. Phys. Lett.*, **20** (2003) 1767.
[16] Fu Y., Yuan N. and Zhang G., *Microwave Opt. Technol. Lett.*, **136-138** (32) 2002.
[17] Zheng L., Jian-Jun X. and Zhi-Fang L., *Chin. Phys. Lett.*, **20** (2003) 516.
[18] Norris R., Hamel J. S. and Nadeau P., *J. Appl. Phys.*, **103** (2008) 104908.
[19] Romero-García V., Fuster-Garcia E., Garcia-Raffi L. M., Sánchez-Pérez J. V. and Uris A., *Phys. Rev. B*, **75** (2007) 224305.
[20] Chen Y.-Y. and Ye Z., *Phys. Rev. E*, **64** (2001) 036616.
[21] García-Pablos D., Sigalas M., de Espinosa F. M., Torres M., Kafesaki M. and García N., *Phys. Rev. Lett.*, **84** (2000) 4349.